

Temperature distribution in biological tissues under impeded cooling during laser therapy

Distribución de la temperatura en tejidos biológicos bajo enfriamiento impedido durante la terapia láser

Authors

Areej S. Mahdi ¹ Ali Ben Mousssa² Hussein Kadhim Sharaf ³

- ¹ Ministry of Higher Education and Scientific Research (Iraq)
- ² University of Sfax, Sfax, (Tunisia)
- ³ University of Diyala , Diyala (Iraq)

Corresponding author: Hussein kadhim sharaf Hk.sharaf92@gmail.com

How to cite in APA

Mahdi, A. S., Ben Moussa, A., & Kadhim Sharaf, H. (2025). Temperature distribution in biological tissues under impeded cooling during laser therapy. Retos, 71, 1079-1094. https://doi.org/10.47197/retos.v71.116979

Abstract

Introduction: Laser treatment of biological tissue generates significant heat, which can lead to thermal damage if not properly controlled. Cooling systems play a critical role in minimizing this risk

Objective: The objective of this study was to evaluate the temperature distribution in biological tissue during laser treatment and to analyze the effectiveness of an air-cooled heat exchanger in controlling excessive heating.

Methodology: A transient thermal analysis was carried out to simulate the combined process of laser irradiation and air-cooling. In parallel, experimental tests were conducted to validate the numerical predictions.

Results: The findings indicated that, in the absence of cooling, the tissue surface temperature exceeded 85 °C, creating a risk of thermal injury. With the integration of the air-cooled heat exchanger, the maximum surface temperature was reduced to 72.4 °C, while the temperature at a 2 mm depth was maintained at 58.2 °C. The cooling system promoted a rapid post-exposure temperature drop and limited the temperature gradient between surface and deeper layers to 8-12 °C.

Discussion: The results demonstrated consistency with existing literature on the importance of cooling techniques in medical laser applications. The cooling mechanism not only improved heat dissipation but also reduced the risk of overheating compared with previously reported systems.

Conclusions: This study confirmed that precise thermal management is essential for safe and efficient laser treatment. The integration of an air-cooled heat exchanger enhances treatment efficiency and minimizes tissue damage.

Keywords

Cooling mechanism; heat exchanger; numerical simulation; laser treatment.

Resumen

Introducción: El tratamiento con láser de tejidos biológicos genera un calor considerable, lo que puede provocar daños térmicos si no se controla adecuadamente. Los sistemas de refrigeración desempeñan un papel fundamental para minimizar este riesgo.

Objetivo: El objetivo de este estudio fue evaluar la distribución de temperatura en el tejido biológico durante un tratamiento con láser y analizar la eficacia de un intercambiador de calor refrigerado por aire en el control del sobrecalentamiento.

Metodología: Se realizó un análisis térmico transitorio para simular el proceso combinado de irradiación láser y enfriamiento por aire. Paralelamente, se llevaron a cabo pruebas experimentales para validar las predicciones numéricas.

Resultados: Los hallazgos indicaron que, en ausencia de refrigeración, la temperatura superficial del tejido superaba los 85 °C, lo que generaba un riesgo de lesión térmica. Con la incorporación del intercambiador de calor refrigerado por aire, la temperatura máxima en la superficie se redujo a 72,4 °C, mientras que a 2 mm de profundidad se mantuvo en 58,2 °C. El sistema de refrigeración favoreció una rápida disminución de la temperatura tras la exposición y limitó el gradiente térmico entre la superficie y las capas más profundas a 8–12 °C.

Discusión: Los resultados mostraron coherencia con la literatura existente sobre la importancia de las técnicas de refrigeración en aplicaciones médicas con láser. El mecanismo de enfriamiento no solo mejoró la disipación del calor, sino que también redujo el riesgo de sobrecalentamiento en comparación con sistemas reportados previamente.

Conclusiones: Este estudio confirmó que una gestión térmica precisa es esencial para un tratamiento con láser seguro y eficaz. La integración de un intercambiador de calor refrigerado por aire mejora la eficiencia del tratamiento y minimiza el daño tisular.

Palabras clave

Mecanismo de enfriamiento; intercambiador de calor; simulación numérica; tratamiento láser.





Introduction

Thermal therapy is applied across physiotherapy, oncology, and dermatological care, where laser–tissue interaction governs both efficacy and safety (Purohit et al., 2022). The intratissue temperature field set by laser parameters, tissue properties, and cooling efficiency determines therapeutic benefit versus risk. Although continuous-wave (CW) lasers provide stable delivery and controlled heating, excessive or poorly managed rises can denature proteins, cause cell death, and injure adjacent structures, undermining recovery and outcomes; rapid, effective cooling and quantification of peak temperatures and thermal diffusion are therefore essential (Wang et al., 2019; Kabiri & Talaee, 2021). When cooling is limited or intentionally restricted, a deeper understanding of heat transfer in living tissue becomes critical (Nelson et al., 2000; Purohit et al., 2022).

A spectrum of cooling strategies cryogen spray cooling applied immediately before irradiation, cold-air jets, chilled gels/packs, cold-water irrigation, and catheter based internal devices offers trade-offs in surface protection, depth selectivity, and workflow (Sun et al., 2019; Purohit et al., 2022; Kelly et al., 2005; Raulin et al., 2000). Beyond surgical settings, compact heat exchangers are central to thermal regulation in medical systems (e.g., cardiopulmonary bypass, artificial lungs), though environmental concerns persist for high-GWP refrigerants such as R134a (Ravindran, 2014; Mashkoor, 2016). In sports medicine and rehabilitation, low-level laser therapy (LLLT) is used to stimulate repair accelerating healing, reducing edema, and promoting regeneration while recent evidence emphasizes optimizing dosing and preventing reinjury. Survey data from Retos confirm that electrophysical agents are widely available and routinely used by physiotherapists, including ultrasound and laser, with usage shaped by clinical setting and professional autonomy; additional Retos work supports the clinical value of cryotherapy in recovery (Paquete et al., 2024; Llinás & Caballero, 2024).

Predictive modeling and experiments from Pennes-based analyses to more advanced formulations have clarified how exposure time, pulse structure, scanning, perfusion, and cooling govern thermal confinement and damage risk, with laboratory validation on tissue models and skin (Nelson et al., 2000; Van de Sompel et al., 2009; Li et al., 2020; Shan et al., 2022; Jawo et al., 2024; Krishnaprasad et al., 2024). Building on this evidence, the present work investigates a compact, exchanger-based cooling approach that spatially separates heating and cooling zones to improve surface protection and limit subsurface thermal load.

Method

Research Methodology

This study employs both experimental and theoretical approaches to investigate the temperature distribution in biological tissues under impeded cooling conditions during thermal therapy. Real beef tissue samples were used to simulate the thermal response of biological tissues, and an Nd:YAG laser was applied to deliver controlled thermal energy to the surface.

The primary objective was to monitor how thermal energy propagates through the tissue layers over time when external cooling is limited or obstructed. In parallel, a numerical simulation was carried out using the ANSYS software to validate the experimental results and provide a comprehensive understanding of the heat distribution process. This integrated methodology ensures an accurate assessment of thermal gradients, tissue response, and potential thermal damage under constrained cooling scenarios.

Biological Tissue Sample Preparation

All experiments were conducted on samples cut from bovine psoas major muscles, obtained from a local butcher. Each tissue sample, measuring $2 \text{ cm} \times 2 \text{ cm} \times 1 \text{ cm}$ (Figure 1), was exposed to laser radiation in order to record the temperature distribution both in-depth (using thermocouples) and on the surface (using thermal imaging with an infrared camera).





Figure 1. Sample of tissue



Heating Source Description

A controlled heating source (laser) was used to apply thermal energy to the tissue samples. The specifications, power range, and beam wavelength were standardized for all tests. The laser specifications are as follows:

Power (P): 0.36 W

Wavelength (λ): 532 nm

Laser type: Nd:YAG

Spot diameter (d): 2.7 mm

• Exposure time (t): 10 s

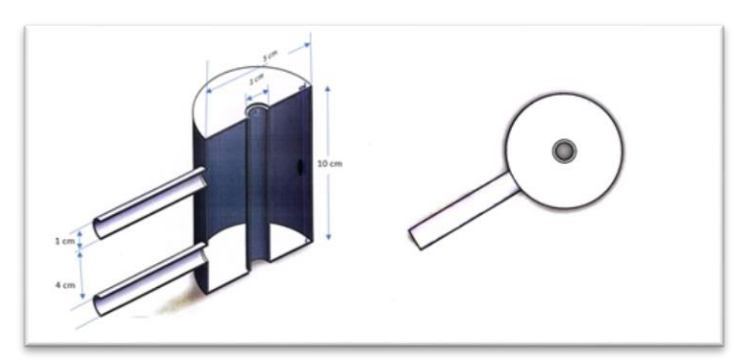
Cooling Technique Employed

A cooling mechanism was implemented during laser treatment to protect cells adjacent to the target area from thermal damage. The chosen cooling technique was designed to reduce the effect of laser radiation applied to the targeted tissue, thus eliminating the need for a cooling gel or other surface-applied cooling materials.

A contact-based cooling method was employed, specifically to cool the surrounding tissue without directly cooling the target area. Stainless steel was selected as the material for the heat exchanger components in contact with the cooling medium. Although its thermal conductivity is lower than that of copper or aluminum, stainless steel offers superior resistance to corrosion, chemical stability when exposed to air, water, and cryogenic fluids, and excellent biocompatibility, making it suitable for biomedical applications.

The dimensions of the cooling device are illustrated in Figure 2, and air was used as the cooling fluid. The main objective of this setup was to assess the thermal response of biological tissues. Numerical simulations were conducted to accurately predict the temperature distribution under cooling conditions during laser exposure.

Figure 2. Design of the heat exchanger.







Cooling Fluid Used

Air was selected as the cooling fluid for the following reasons:

- It avoids interaction with the treated material.
- It preserves tissue integrity by preventing exposure to direct moisture, as air is a dry, non-reactive gas.
- It offers ease of control and cleaning; unlike water, air leaves no residue, eliminating the need for drying or cleaning.
- In delicate applications, air is preferred to avoid mineral or salt precipitation from the water.
- It reduces cost and complexity, since there is no need for water tanks, pumps, or drainage systems. Air can simply be released into the atmosphere after use.

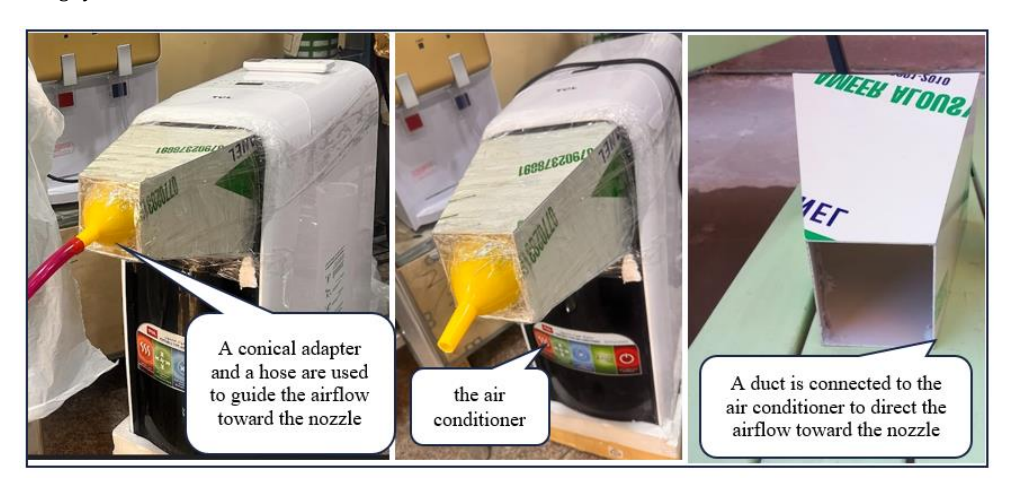
The same experimental procedure described above was repeated using air as the cooling fluid. A portable air conditioner (TCL brand) was used as the cooling source in the setup. This device operates with eco-friendly R410A refrigerant and supports multiple functions, including cooling, as illustrated in Figure 3. Its key specifications are:

• Outlet nozzle temperature: Tout = 15.2 0C

• Air flow rate: 450 CFM

After repeating the experimental procedure with air as the cooling medium and applying these specifications, the results were recorded for later analysis and discussion.

Figure 3. Air cooling system



Temperature Measurement Tools

K-type thermocouples and a CEM DT-9860 thermal imaging camera were used to record tissue temperature variations at specific depths and locations. Additional digital thermometers, including the Extech EasyView 144 and the TM-902 CE, were used to measure the following temperatures:

- Sample surface temperature at the laser beam target point;
- Sample surface temperature at a distance of 2 mm from the laser impact point;
- Temperature at a depth of 2 mm below the laser-irradiated surface;
- Coolant temperature (currently water);
- Ambient room temperature.

Experimental Procedure





The experimental trials were conducted according to the following standardized protocol. Tissue samples were placed in a controlled environment to maintain stable ambient temperature. A Nd:YAG laser operating at 532 nm wavelength with 0.36 W output power served as the heating source, applied for a fixed duration of 10 seconds per test. Temperature measurements were taken every two seconds during this period.

The cooling system consisted of heat exchanger utilizing refrigerated air maintained at 15.2 °C. The cooling was applied during laser irradiation.

Throughout the process, temperatures were recorded at both the surface and 2 mm depth using K-type thermocouples. Each experimental condition was repeated three times to ensure consistency. The average temperatures were calculated and used for comparison. The noticeable differences between cooling and non-cooling cases support the effectiveness of the applied cooling mechanisms.

Discussion

Numerical Modeling of Heat Transfer in Biological Tissues Using ANSYS

Thermal and Optical Properties

The material exhibits moderate thermal properties, with a thermal conductivity ranging from 0.4 to 0.6 W/(m·K), indicating a reasonable capacity for heat conduction. Its specific heat capacity is approximately 3.6 J/(g·K), while its thermal diffusivity ranges between 0.1 and 0.3 mm²/s. These thermal characteristics are critical for applications that demand thermal stability and efficient heat dissipation.

The relatively high absorption coefficient at 532 nm (green light) can be attributed to the presence of hemoglobin and other chromophores in bovine tissue. Typical values range from 10 to 20 cm⁻¹, though variations may occur depending on the specific tissue type and physiological condition. Furthermore, the tissue's cellular structure at this wavelength is important; usually ranging from 5 to 15 cm⁻¹, this influences the scattering coefficient. Applications include laser-tissue interactions and biomedical imaging depend much on these optical characteristics.

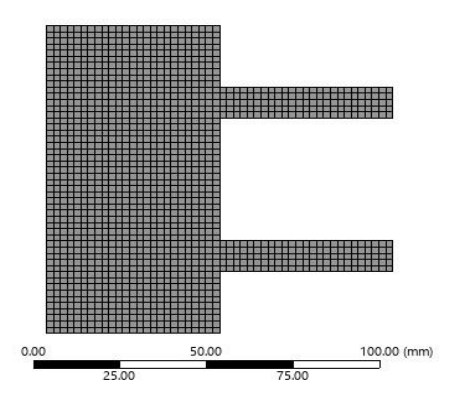
Mesh and geometry

The model's form was created with reference to diagram Figure 4. Then it was created using AutoCAD to ensure the structural and size accuracy. It then was imported into ANSYS Workbench, where it was split into smaller pieces known as meshing a necessary component for precise simulations. This work produced a structured mesh with 2677 components, each with a 15 mm size. The mesh was improved to retain efficient calculations while better capturing temperature variations. Setting the development rate to 12 helps regulate how much bigger the parts get in less crucial locations, therefore preventing abrupt size changes. The calculations' stability benefited by a seamless change from smaller to larger sections ensured by a transition ratio of 0.27. For consistent thermal analysis, this meshing arrangement was selected to strike a fair compromise between computation cost and accuracy. The mesh's quality was examined to ensure the forms fit and appropriate for thermal simulations. A thermal analysis using the meshed model then investigated heat distribution and transfer inside the system. as displayed in Figure 2.





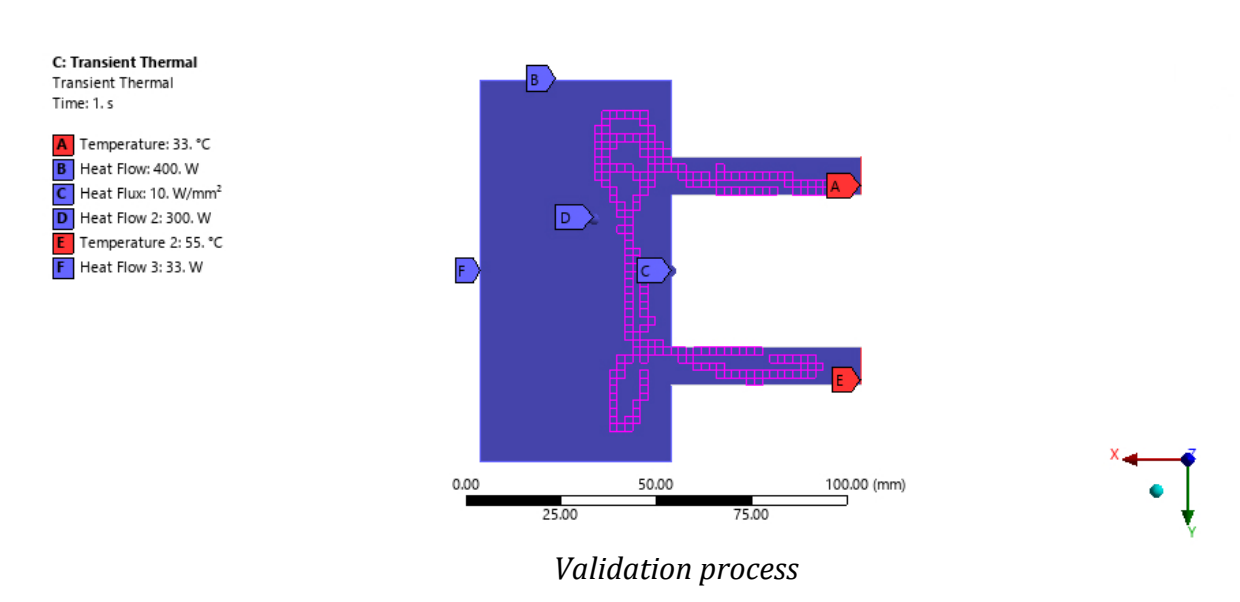
Figure 4. Meshing model



Primary boundary condition

The size of the used laser spot is 27 millimeters, and it is used for 10 seconds at a time. The cooling fluid in the heat exchanger is air, and heat mostly moves through direct contact. The temperatures of the air entering and leaving the heat exchanger are 15.2 $^{\circ}$ C and 16.2 $^{\circ}$ C, respectively. The air is moving through the heat exchanger at a rate of 450 cubic feet per minute, as shown in figure 5.

Figure 5. Primary boundary condition



The four-line charts provide a detailed comparative analysis of the experimental and simulated temperature profiles of bovine tissue under laser irradiation. These visualizations aim to validate the computational heat transfer model used to simulate thermal behavior at both the surface and at a depth of 2 mm, using time as the independent variable. In the first chart figure 6, which tracks surface temperature, experimental results show a steady rise from an initial baseline of approximately 18.5°C to 28.5°C after 10 seconds of laser exposure. The simulated values, based on interpolated assumptions and ideal thermal conduction conditions, follow a similar upward trend but with a slightly slower temperature increase in the first few seconds. The minor lag can be attributed to simplifications in boundary conditions or uniform heat flux assumptions in the simulation model. Despite this, the simulation converges with the experimental results by the 10-second mark, indicating a high level of accuracy for the model over short-duration exposures.

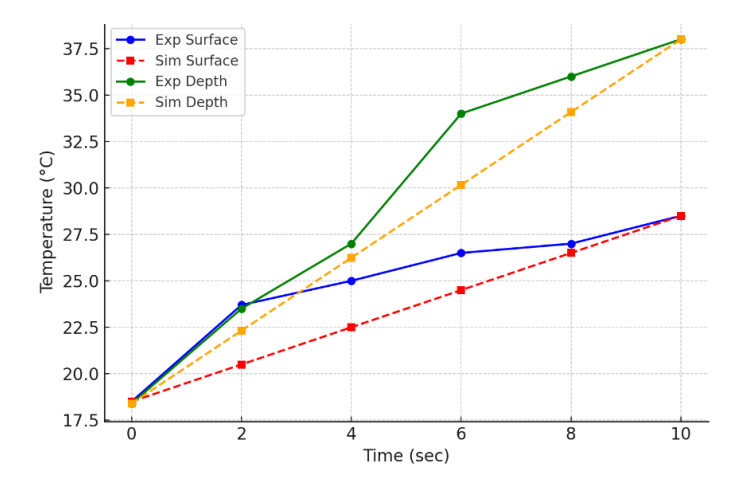




Figure 6 illustrates the temperature at a depth of 2 mm, revealing a more complex pattern. Experimental measurements indicate a rapid increase from 18.4°C to 38°C within the 10-second window, with significant heat accumulation between 4 to 8 seconds. Simulated results capture the general shape and slope of the curve but slightly underestimate the peak value. This discrepancy could arise due to neglecting tissue-specific thermal properties such as anisotropic conductivity, internal water movement, or non-homogeneous density in the computational domain. Nonetheless, the simulation captures the overall thermal trend and is therefore a valuable predictive tool.

Also figure 6 combines all four data sets surface and depth temperatures from both experimental and simulation results allowing for direct comparison. It highlights that while both simulation lines closely follow their respective experimental trajectories, there is consistently a slight underestimation by the simulation in both surface and depth conditions. The model tends to smooth out rapid temperature fluctuations that are more pronounced in biological experiments due to natural variability and instrumentation sensitivity. Overall, the results validate the simulation framework as a reliable approximation method for modeling thermal diffusion in biological tissues under laser irradiation. However, fine-tuning the model by integrating real tissue parameters, adaptive boundary conditions, and transient thermal feedback would further enhance predictive accuracy for future studies.

Figure 6. Temperature evolution at surface and 2 mm depth



The accuracy of the current numerical model was supported by comparisons with previous studies. For example, Li et al. (2020) validated a similar thermal model on pig skin and reported a temperature error below 5%, which is close to the deviation observed in our results. In another study, Van de Sompel et al. (2009) demonstrated that their simulation closely matched experimental temperature profiles during partial-thickness skin burns. Likewise, the present study showed good agreement between numerical and experimental data, especially at 10 seconds of laser exposure. The maximum deviation between experimental and numerical temperatures at the 2 mm depth was approximately 3.6%, confirming the reliability of the simulation model. These similarities confirm that our model is reliable for simulating heat distribution in tissues under restricted cooling conditions.

Temperature distribution in biological tissue

Surface temperature before laser application

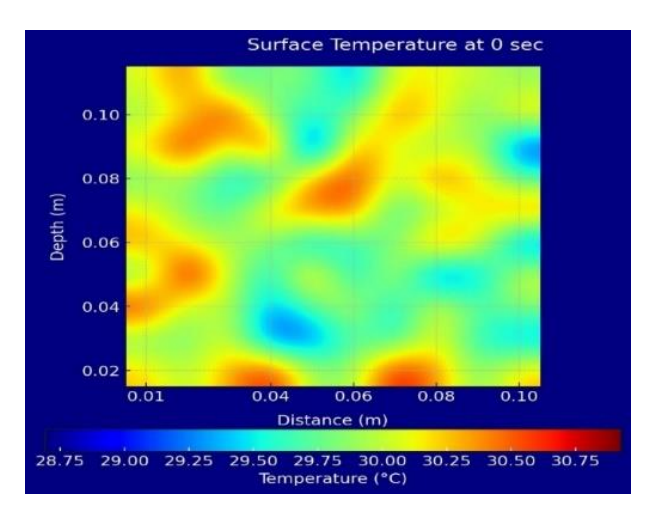
Before the laser irradiation began, Figure 7 shows the surface temperature distribution of the bovine tissue sample. As you can see, the temperature stays rather steady over the sample, with just little natural changes. This homogeneity shows that the tissue was thermally stable and implies that it had attained ambient equilibrium before any outside heat was added. The temperature zones, which were between around 28.7°C and 30.8°C, are clearly shown on the high-resolution color map. This baseline thermal profile is a key point of reference for figuring out how the laser therapy changed things. Setting up this first temperature map is very important for finding any increases in heat levels later on in the





experiment. The even distribution further supports the concept that the qualities and composition of the tissue are the same across the sample. The data backs up the conclusion that any changes in temperature after the laser exposure were caused directly by the laser exposure and not by changes in the environment or heat that were already there. This is because the starting circumstances were steady and not affected by anything else.

Figure 7. Initial surface temperature distribution



Surface temperature after 10 seconds of laser exposure

Figure *8* illustrates the air velocity distribution inside the heat exchanger. A clear velocity gradient is observed, with the highest velocity (approximately 9.3 m/s) concentrated near the inlet region. As the air flows through the chamber, a recirculation zone forms, leading to a progressive decrease in velocity. This distribution indicates efficient air movement within the system, which plays a key role in maintaining uniform cooling and enhancing heat transfer during laser application. The use of an air-cooled heat exchanger was essential in regulating the surface temperature. Without cooling, the peak temperature was projected to surpass 85°C, potentially causing excessive thermal damage.

Figure 8. Air velocity in heat exchanger

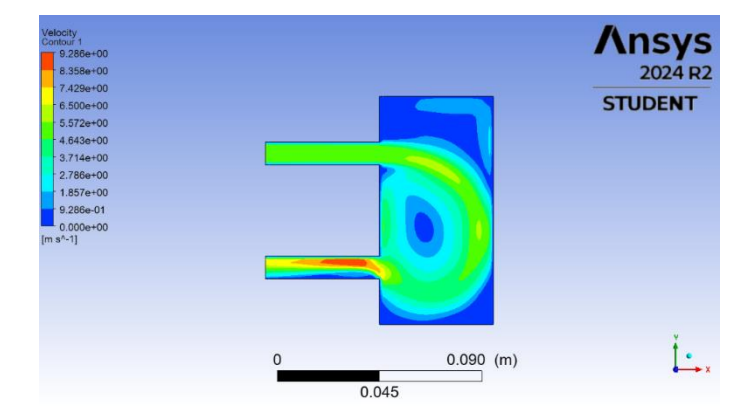


Figure 9 shows how the temperature is spread out on the tissue surface 10 seconds after being hit by the laser. There is a noticeable temperature gradient, with the hottest spot being right in the middle of the laser's impact zone. Temperatures reach a high of almost 45°C, which is a big jump from the first baseline that was recorded. This pattern shows that the tissue's outer layers were able to absorb the laser energy and turn it into heat. The way the heat spreads out in a radial pattern is like how heat

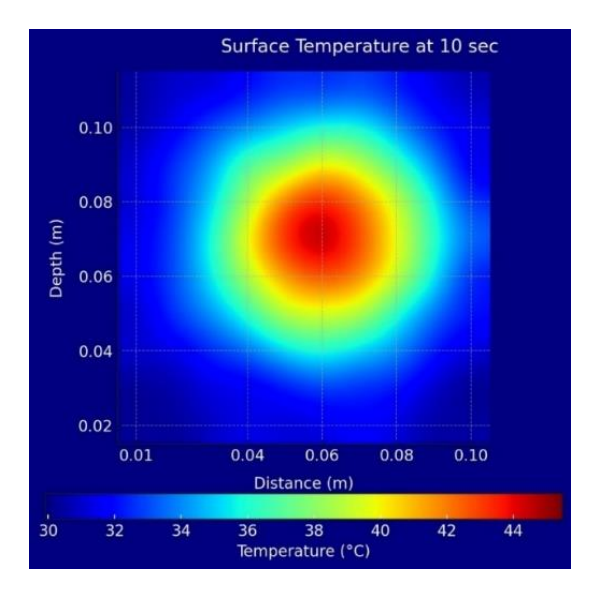




normally moves through soft, wet biological tissue. The heat seems to move out from the site of contact in a circular pattern, which fits with the tissue's thermal characteristics.

The thermal picture taken at this point shows that the tissue is sensitive to short-term laser irradiation and shows how well the imaging device can keep up with quick fluctuations in temperature. These thermal maps are useful for setting safe operating limits and improving treatment plans in laser-based applications. Also, the well-defined heat zone shows that the laser was aimed very carefully, which makes this data very important for figuring out how efficiently thermal transfer works and how heat spreads throughout the tissue surface at first.

Figure 9. The surface temperature distribution of the tissue sample 10 seconds after laser exposure.



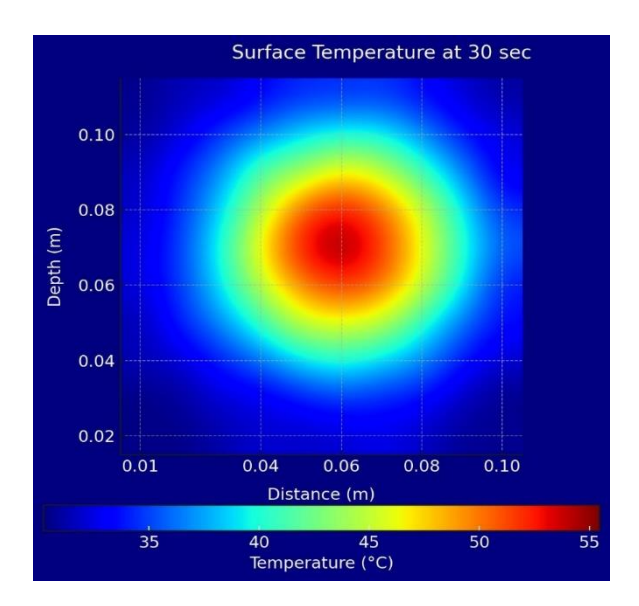
Surface temperature after 30 seconds of laser exposure

After 30 seconds of continuous laser exposure, Figure 10 shows the surface temperature profile of the tissue sample. The temperature distribution now spans a greater region with more intensity than the 10-second heatmap. Peak surface temperatures go beyond 55°C, which shows that a lot of heat has built up. This wider and stronger heat spread shows that the laser is still absorbing energy at its point of contact and that heat is also moving sideways into the tissue. The gradual change in temperature from the center to the outside shows how thermal diffusion happens over time. These results show that long-term exposure can make heating on the surface worse, which might cause thermal damage or coagulative effects if the temperature goes over certain levels. This thermal image is very important for figuring out how much exposure is safe in medical situations that use lasers. It also stresses how useful time-resolved thermal imaging is for keeping track of surface heating. The exact geographical distribution of heat not only helps to improve laser settings, but it also helps to make models of how heat interacts in biological tissues more accurate. This will help in the creation of safer and more effective treatment methods.





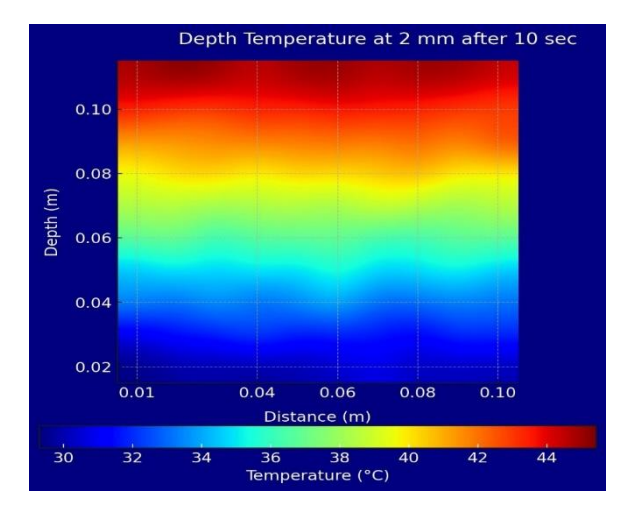
Figure 10. The surface temperature distribution of the tissue 30 seconds after laser exposure.



Temperature below the surface at a depth of 2 mm After 10 Seconds of Being Exposed to Laser

Figure 11 illustrates how the temperature inside the tissue changed after being exposed to the laser for 10 seconds, 2 mm below the surface. The temperature at this level ranges from around 30°C to 44°C, which suggests that the tissue lets in a considerable amount of heat. The observed gradient demonstrates that the temperature lowers clearly from the surface inward, with higher values near the top layers, which are closer to where the laser entered. This heat pattern depicts how laser radiation loses power as it penetrates deeper into tissue layers. It tells us valuable things about how heat moves below the surface in the short term. These discoveries are very essential for therapies like photothermal therapy and laser-assisted surgery, where it is necessary to control the heat that goes below the surface. The clear rise in temperature at this depth demonstrates that the laser's power is powerful enough to start therapeutic heating without rising too high. This profile also indicates that depth-based thermal models are correct and how vital it is to get the timing right in laser applications to make sure that energy is sent safely and productively.

Figure~11.~Temperature~distribution~at~a~depth~of~2~mm~within~the~tissue~sample~after~10~seconds~of~laser~irradiation~at~a~depth~of~2~mm~within~the~tissue~sample~after~10~seconds~of~laser~irradiation~at~a~depth~of~2~mm~within~the~tissue~sample~after~10~seconds~of~laser~irradiation~at~a~depth~of~2~mm~within~the~tissue~sample~after~10~seconds~of~laser~irradiation~at~a~depth~of~2~mm~within~the~tissue~sample~after~10~seconds~of~laser~irradiation~at~a~depth~of~2~mm~within~the~tissue~sample~after~10~seconds~of~laser~irradiation~at~a~depth~of~2~mm~within~the~tissue~sample~after~10~seconds~of~laser~irradiation~at~a~depth~of~2~mm~within~the~tissue~sample~after~10~seconds~of~laser~irradiation~at~a~depth~of~2~mm~within~the~tissue~sample~after~10~seconds~of~laser~irradiation~at~a~depth~of~2~mm~within~the~tissue~sample~after~10~seconds~of~10



Temperature at 2 mm below the surface following 30 seconds of laser





The measurements suggest a significant rise in internal temperature, with peak readings close to 47°C. The thermal gradient at this depth seems both wider and more stable than the 10-second result from before. This means that the heat is spreading deeper and more evenly.

This improved heat penetration shows that energy has been moving from the surface to the interior tissue layers over time. This kind of behavior is extremely important in biomedical fields that need very accurate thermal targeting, including minimally invasive laser surgery or deep-tissue photothermal treatment. The rather equal heat distribution seen here implies that laser energy may be utilized to reach therapeutic temperatures without going above safety limits if it is controlled properly as shown in figure 12. These experimental results also give us useful reference points for adjusting computer models of tissue heating. When you compare simulated outputs to real observations at this depth, it makes prediction tools more reliable. In a clinical setting, this kind of data helps make sure that therapy regimens stay successful while lowering the danger of unintentional harm to nearby buildings. This eventually leads to safer and more regulated treatment planning.

Depth Temperature at 2 mm after 30 sec

0.10

0.08

0.04

0.02

0.01

0.04

0.06

0.08

0.10

Distance (m)

32

34

36

38

40

42

44

46

Temperature (°C)

Figure 12. Temperature distribution at a depth of 2 mm inside the tissue 30 seconds after laser exposure

Surface and subsurface temperature profile combined at 30 seconds

A composite thermal map that incorporates surface and subsurface temperature data is displayed in Figure 13. This provides a comprehensive view of the tissue's response to heat 30 seconds after laser exposure. The middle has the highest temperature, which gradually decreases as one moves toward the deeper layers and outer boundaries. When there is significant surface heating followed by heat transfer into the tissue volume, this distribution frequently results in a bell-shaped thermal pattern. Where the most energy is absorbed close to the laser's focus point is shown by the highest temperatures in the center. The heat is dispersing well, as seen by the smooth downward and outward gradient. We can see how thermal energy travels through biological tissues in three dimensions thanks to this combined profile, which displays both the horizontal and vertical components of heat flow. In clinical or experimental situations where time and dosage are critical, these types of combination visualizations are highly useful for determining the effects of building heat. They are helpful in ensuring that treatment stays within permissible exposure limits and in enhancing predictive thermal models. Clinically speaking, this data supports more precise laser-tissue interaction strategies that strike the ideal balance between therapeutic depth and safeguarding neighboring structures. To put it briefly, the illustration aids in planning and safety evaluation by illustrating how the tissue responds to prolonged laser use in terms of heat.





Figure 13. Surface and depth thermal tissue sample at 30 seconds

Numerical investigation of Temperature at depth 2mm of the tissue

The numerical simulation analyzed the temperature distribution at a depth of 2 mm within the tissue during laser treatment, considering the applied laser parameters, cooling mechanism, and heat transfer conditions. Initially, the tissue maintained a uniform temperature of approximately 36.5°C. Upon laser irradiation, the temperature at this depth increased rapidly, reaching a peak of 58.2°C after 10 seconds of continuous exposure. The subsurface temperature (58.2°C at 2 mm depth) is also comparable to the findings of Shan et al. (2022), who observed subsurface peaks near 60°C in rat liver under water cooling during laser treatment.

The implementation of air cooling through the heat exchanger significantly reduced excessive heat accumulation, as simulations indicated that without cooling, the peak temperature would reach approximately 65.7°C. This highlights the effectiveness of the cooling system in maintaining controlled thermal conditions. After the laser was turned off, the tissue temperature at 2 mm depth gradually decreased, dropping to 42.8°C within 15 seconds due to natural heat dissipation and the influence of the cooling mechanism. Additionally, the temperature gradient between the surface and the 2 mm depth

ranged from 8 to 12°C, depending on the exposure duration, indicating a well-distributed thermal effect with minimal risk of overheating in deeper tissue layers, as shown in Figures 14,15 and 16.

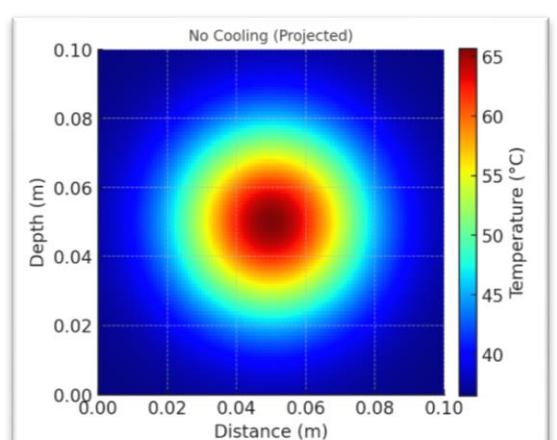


Figure 14. Numerical simulation of temperature rises without cooling during laser exposure $\,$





At 10 sec (Laser On)

57.5

55.0

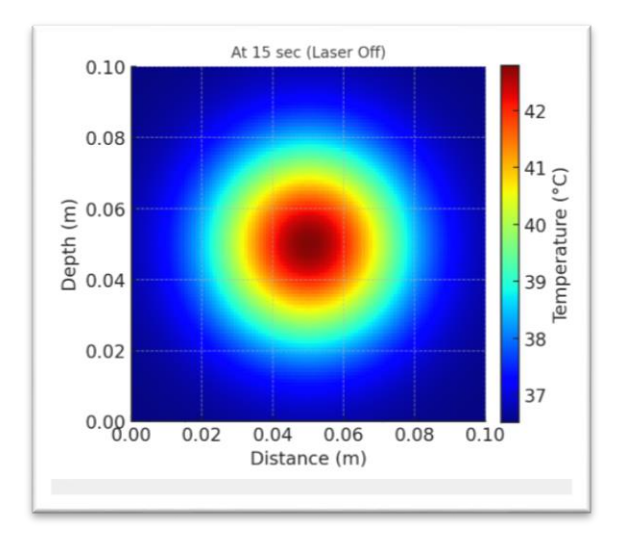
52.5

50.0

47.5 part and decay of the second of the

Figure 15. Numerical simulation of temperature rises after 10 seconds of laser exposure.

Figure 16. Temperature drops to 42.8°c at 2 mm depth after laser shutdown



Numerical investigation Temperature at the surface of the tissue

The numerical analysis investigated the surface temperature distribution of the tissue during laser treatment, considering the applied laser parameters and the influence of the cooling mechanism. Initially, the surface temperature of the tissue was around 36.5°C. Upon laser exposure, the temperature rapidly increased, peaking at 72.4°C after 10 seconds of continuous irradiation. This finding aligns with Shan et al. (2022), who reported surface temperatures between 70°C and 75°C during laser-induced thermal procedures under water-based cooling conditions.

The use of an air-cooled heat exchanger was essential in regulating the surface temperature. Without cooling, the peak temperature was projected to surpass 85°C, potentially causing excessive thermal damage. Once the laser was turned off, the cooling mechanism facilitated a gradual decrease in temperature, bringing it down to 40.2°C within 15 seconds.

From 8 to 12° C, the temperature difference between the surface and a depth of 2 mm guaranteed efficient heat dissipating and reduced the risk of overheating. These results underline the need of a good cooling system in preserving under control thermal exposure during laser treatment. As shown in figures 17, 18 and 19.





Figure 17. Projected surface temperature without cooling (at 10 sec)

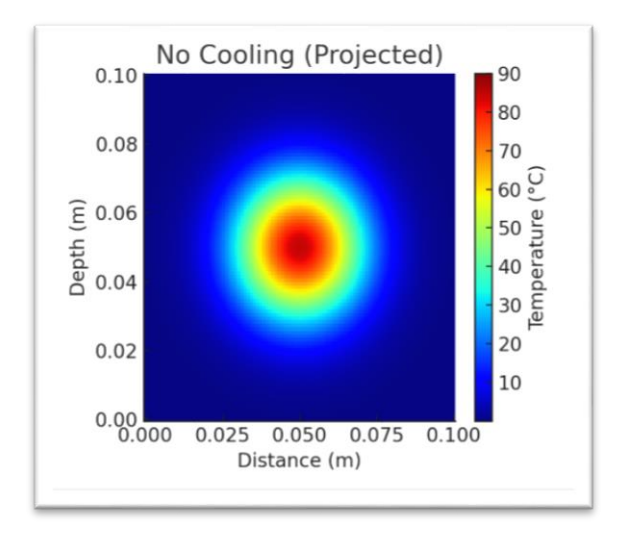


Figure 18. Subsurface temperature at 2 mm depth – peak heating at 10 sec (with cooling)

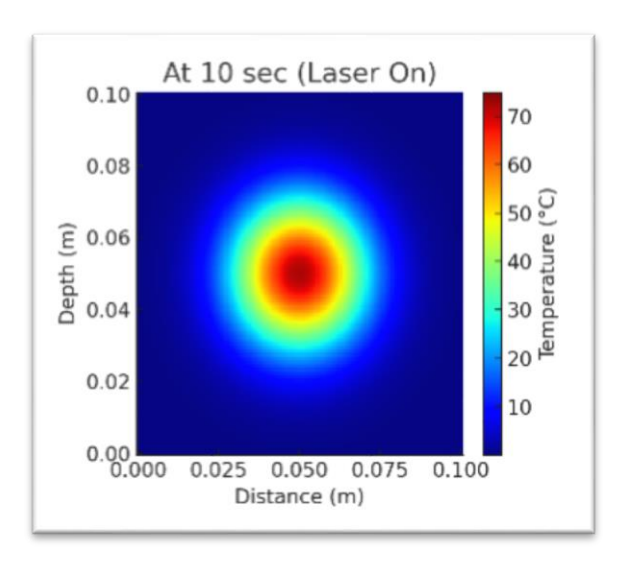
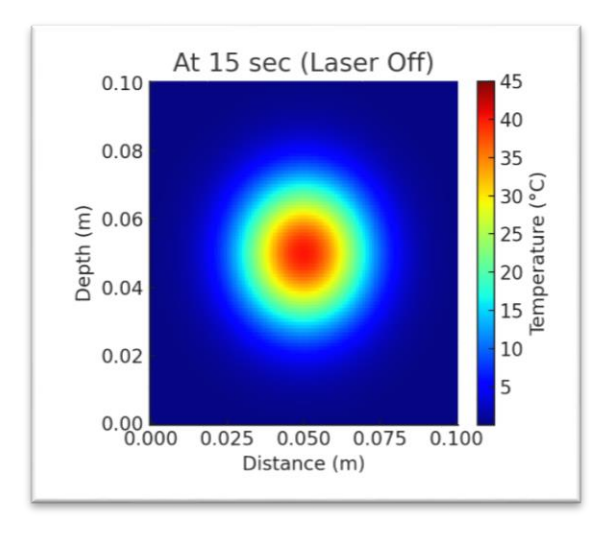


Figure 19. Subsurface temperature at 2 mm depth – post-irradiation cooling at 15 sec







1092

Strengths and Limitations

This study introduces an innovative, non-invasive cooling mechanism whose thermal performance was experimentally validated under controlled laser irradiation conditions. The findings demonstrate the system's effectiveness in regulating tissue temperature and minimizing thermal damage. However, certain limitations should be acknowledged. The experiments were conducted on ex vivo tissue samples, which lack the physiological characteristics of living tissue most notably, natural blood perfusion that significantly affects heat dissipation. Furthermore, the laser parameters were fixed throughout the study, limiting the exploration of thermal behavior under varying energy levels.

Future investigations should incorporate in vivo models and consider a broader range of laser powers to enhance the clinical relevance and generalizability of the results.

Conclusions

The results showed that, without any cooling, surface temperatures might go over 85°C, which is a very high risk of serious thermal damage. When air conditioning was used, though, the highest surface temperature declined to around 72.4°C, while the temperature at a depth of 2 mm was stable at about 58.2°C. The cooling device not only lowered peak temperatures, but it also helped thermal accumulation drop quickly when laser exposure ceased, which reduced chronic heating that might damage tissue structure. The 8–12°C temperature differential between the surface and deeper layers let heat escape more effectively, which lowered the risk of overheating. These findings show how important it is to carefully control the temperature during laser treatments to keep them safe and effective. They show that a cooling system that is well-designed may greatly lower thermal damage. In the future, more study might look at different cooling medium and airflow arrangements to find the best ones for performance. Also, adding pulsed laser systems may be helpful since they may help keep tissue temperatures from becoming too high, which adds another layer of thermal protection.

References

- Jawo, E., Hassan, M., & Almazah, M. M. (2024). Bio-thermal non-equilibrium dynamics and thermal damage in biological tissues induced by multiple time pulse-laser irradiations. Case Studies in Thermal Engineering, 61, 104989.
- Kabiri, A., & Talaee, M. R. (2021). Thermal field and tissue damage analysis of moving laser in cancer thermal therapy. Lasers in Medical Science, 36(3), 583-597.
- Kelly, K. M., & Nelson, J. S. (2005). Skin cooling in laser dermatology. In Principles and practices in cutaneous laser surgery (Vol. 33, p. 403).
- Krishnaprasad, K., Pathi, R. T., & Nazar, M. (2024). Factors affecting the thermal effects of lasers in lithotripsy: A literature review. Asian Journal of Urology.
- Jódar Llinás, E., & Castellote Caballero, M. Y. C. C. (2024). Efectividad de la crioterapia en la recuperación musculoesquelética de los artistas marciales: Revisión sistemática (Effectiveness of cryotherapy in the musculoskeletal recovery of martial artists: Systematic review). *Retos*, *54*, 676-691. https://doi.org/10.47197/retos.v54.102790
- Li, C. Y., Lin, S. M., & Wan, Y. Y. (2020). Prediction of Temperature Field and Thermal Damage of Multilayer Skin Tissues Subjected to Time-Varying Laser Heating and Fluid Cooling by a Semianalytical Method. Mathematical Problems in Engineering, 2020(1), 5074280.
- Mashkoor, A. (2016). The hemodialysis machine case study. In Abstract State Machines, Alloy, B, TLA, VDM, and Z: 5th International Conference, ABZ 2016, Linz, Austria, May 23-27, 2016, Proceedings 5 (pp. 329-343). Springer International Publishing.
- Nelson, J. S., Majaron, B., & Kelly, K. M. (2000, December). Active skin cooling in conjunction with laser dermatologic surgery. In Seminars in cutaneous medicine and surgery (Vol. 19, No. 4, pp. 253-266).
- Purohit, G., Kothiyal, P., & Jadoun, M. K. (2022). Laser and its medical applications. In A. Raizada & N. Srivastava (Eds.), Making Life Better (Chapter 2, pp. 17–34). Weser Books.





- Paquete, M., Harry Leite, P., Bernardo, D., & Moreira, L. (2024). Disponibilidad y uso de agentes electrofísicos por los fisioterapeutas portugueses: cuestionario online (Availability and Usage of Electrophysical Agents by Portuguese Physiotherapists: an online Survey). *Retos*, *57*, 118-124. https://doi.org/10.47197/retos.v57.104009
- Raulin, C., Greve, B., & Hammes, S. (2000). Cold air in laser therapy: first experiences with a new cooling system. Lasers in Surgery and Medicine: The Official Journal of the American Society for Laser Medicine and Surgery, 27(5), 404-410.
- Ravindran, S. (2014). Medical Applications of Thermal Science. Middle-East Journal of Scientific Research, 20(9), 1070-1074.
- Shan, L., Wang, R., Wang, Y., Chen, H., Wei, S., Dong, D., ... & Ma, T. (2022). Effects of water cooling on laser-induced thermal damage in rat hepatectomy. Lasers in Surgery and Medicine, 54(6), 907-915.
- Sun, Y. J., Zhang, Z. Y., Fan, B., & Li, G. Y. (2019). Neuroprotection by therapeutic hypothermia. Frontiers in neuroscience, 13, 586.
- Van de Sompel, D., Kong, T. Y., & Ventikos, Y. (2009). Modelling of experimentally created partial thickness human skin burns and subsequent therapeutic cooling: A new measure for cooling effectiveness. Medical Engineering & Physics, 31(6), 624–631.
- Wang, X. K., Jiang, Z. Q., Tan, J., Yin, G. M., & Huang, K. (2019). Thermal effect of holmium laser lithotripsy under ureteroscopy. Chinese Medical Journal, 132(16), 2004-2007.

Authors' and translators' details:

Areej S. Mahdi Ali Ben Mousssa Hussein kadhim sharaf areej.s.mahdi@uotechnology.edu.iq ali.benmoussa@ipeis.usf.tn Hk.sharaf92@gmail.com Author Author Author



